Journal of Structural Chemistry. Vol. 56, No. 1, pp. 67-76, 2015.

STRUCTURE OF DIMERS OF GLYCYRRHIZIC ACID IN WATER AND THEIR COMPLEXES WITH CHOLESTEROL: MOLECULAR DYNAMICS SIMULATION

M. V. Zelikman[1, 2], A. V. Kim[1, 2], N. N. Medvedev[1, 2], O. Yu. Selyutina[1, 2], and N. E. Polyakov[2]

UDC 544.353.3:544.272

The molecular dynamics simulation of dimers of glycyrrhizic acid (GA) arising from the spontaneous meeting of two GA molecules in water is performed. Shown that the molecules in the dimer are quite close to each other, there is no place between them where another molecule (including water molecule) could fit. The relatively stable structures of dimers are found, which are characterized by the specific values of angles between the terpene skeletons of GA molecules and sugar ends. Due to thermal motion, the spontaneous transitions between these structures occur. The insertion of a molecule of cholesterol in the solution showed that the associates formed from two GA molecules and one cholesterol molecule are, as a rule, one of stable GA dimers with the attached cholesterol molecule.

DOI: 10.1134/S0022476615010102

Keywords: molecular dynamics simulation, aqueous solutions, glycyrrhizic acid, cholesterol, structure of associates, guest-host mechanism.

INTRODUCTION

Glycyrrhizic acid (triterpene saponin from the extract of licorice root) exhibits a broad spectrum of biological activity and has long been used to treat and prevent different diseases [1]. To date, a large volume of experimental evidence is accumulated indicating that, besides its own biological activity, GA is able to enhance bioavailability of other drugs in case of their joint administration and improves the solubility of many hydrophobic medicinal compounds [2, 3]. The molecular mechanism of this GA action is yet not understood despite a variety of physicochemical studies. It was established experimentally that due to the presence of hydrophilic and hydrophobic parts, GA molecules can form stable complexes with many organic molecules [3-12]. The stability constant of these complexes exceeds that for analogous complexes of cyclodextrins. It is also known that GA shows properties typical of micelle-forming substances [11-17]. It can form self-associates in aqueous and water-alcohol solutions [3, 11], which composition depends on the GA concentration. However, the structure of these aggregates and mechanism of their formation are also not understood. There are indications that stoichiometry of GA complexes with various substances at low concentrations is usually 2:1 or 4:1 (GA:guest molecule). Furthermore, it has been suggested that GA bonding with membrane cholesterol can play an important role in the mechanism of its biological activity [18]. The formation of GA complexes with cholesterol in solution was proved by NMR relaxation [18].

[1]Novosibirsk State Research University, Russia. [2]Voevodskii Institute of Chemical Kinetics and Combustion, Siberian Branch, Russian Academy of Sciences, Novosibirsk, Russia; nikmed@kinetics.nsc.ru. Translated from *Zhurnal Strukturnoi Khimii*, Vol. 56, No. 1, pp. 73-82, January-February, 2015. Original article submitted May 16, 2014.

We studied the GA solutions by the molecular dynamics method. In the literature, there are few works on the simulation of glycyrrhizic acid. Molecular dynamics simulation was used in [19]. A GA molecule is there considered as an inhibitor of Ku protein responsible for DNA repair (this protein can be potentially applied as antitumor agent). The researches showed that glycyrrhizin (and macedonoside C) is the best (from the whole database of the substances of traditional Chinese medicine) suitable for the reaction center of this protein. The protein–ligand interaction was simulated in the *NVE* ensemble for 10 ns. It appeared that during this time interval the complex does not decompose, but conversely, stabilizes. In [20], the associates of GA molecules using quantum chemical calculations were studied. It was shown that in vacuum (without regard to the solvent) the most favorable bimolecular GA complex has a head-to-tail structure type. It is stabilized by hydrogen bonds between the GA molecules. The authors note the presence of an internal void in this structure suitable for insertion of commensurate guest molecules. To assess the solvent effect, the authors added 6 water molecules, which fit within the void. Unfortunately, based on this simulation it is difficult to talk about the structure of the complex in solution. The influence of the surrounding water on the structure of bimolecular associate can be much greater than interaction between the GA molecules calculated in [20]. A cluster consisting of six GA molecules organized in 6-membered rings was also considered. Within this cluster, there is a wide internal void. However, again, this does not mean that these specific clusters would exist in solution.

In this paper, we simulated the spontaneous formation of GA dimers in water and its associates with cholesterol of the composition 2:1 and analyzed their structure in detail.

SIMULATION

We performed a classical molecular dynamics simulation using the Gromacs software [21]. The equilibrium paths of the models under study were obtained in the *NPT* ensemble at a pressure of 1 bar and a temperature of 300 K. We used a Nose–Hoover thermostat [22] in combination with a Parrinello–Rahman barostat [23]. The electrostatic interaction was calculated using the accelerated Ewald summation technique [24] with fourth-order interpolation. A simulation step was 2 fs. For the structural analysis, the model configurations were recorded every 2 ps. We failed to find a ready-made molecular dynamics representation of GA molecule in the literature. To obtain the file with GA molecular topology, the Automatic Topology Builder (ATB) was used [25] with the GROMOS force field. The ATB provides a multistage optimization of the parameters involving quantum-mechanical calculations to determine the charge distribution on a molecule. The coordinates of the initial GA configuration were taken from the PDB database. A ready-made molecule of cholesterol was taken from the ATB database [26]. For water, the Tip4p-Ew model was used.

A model of GA solution in water is a model box with two GA molecules surrounded by about 7000 water molecules. The model of GA solution with cholesterol also contains two GA molecules and one cholesterol molecule surrounded by approximately 6970 water molecules in the model box of about the same volume. We carried out 30 independent runs with a duration of 30 ns for each model. As it turned out in our calculations, the molecules stuck together do not decouple any more. To confirm this, some runs lasted for more than 100 ns. Each run started from its own independent initial configuration where the dissolved molecules were separated by as large distance as possible and the orientations on the molecules were randomly selected (Fig. 1).

Due to diffusive motion, the molecules could meet and form an associate. For the model of GA solution, in 20 of 30 runs a dimer formed, and in the other 10 runs the molecules did not have time to meet during simulation. For the model of GA solution with cholesterol, in 25 runs the aggregates of the composition 2:1 formed, while in the other five runs only bimolecular associates formed: in three cases, the GA dimers appeared, and in two cases, an aggregate consisting of a GA molecule with cholesterol (see below).

FINDING A DIMER

A time of dimer formation is well fixed by the value of van der Waals interaction between GA molecules. The Gromacs software provides the calculation of the interaction energy between the given groups of atoms. In this case, we

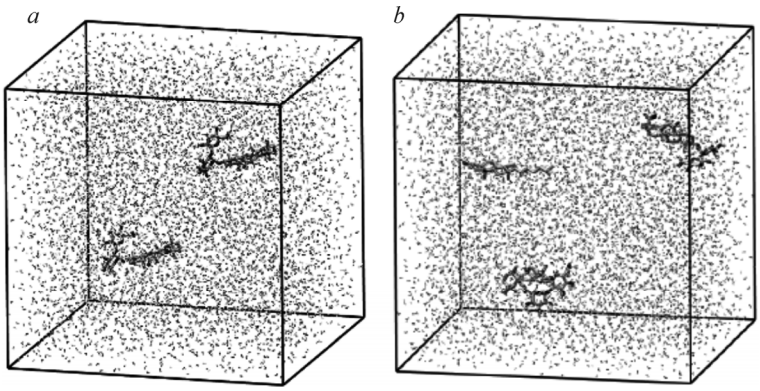

Fig. 1. Examples of initial configurations: the model with two GA molecules (the molecule skeletons are shown) surrounded by water molecules (shown by dots) (*a*); the model with two GA molecules and one cholesterol molecule (*b*).

calculated the Lennard–Jones interaction energy E_{LJ} between all atoms of GA molecules not bound by covalent bonds. This energy does not include the molecular interaction with water and the electrostatic interaction between the molecules and water, but it proves to be a good measure for determining the time of molecular sticking. The E_{LJ} value experiences an abrupt jump when the molecules meet; see the top curve in Fig. 2. (Note that E_{LJ} slightly differs from the Lennard–Jones interaction energy between different GA molecules, since in such a calculation the Gromacs also takes into account the Lennard–Jones interaction between the remote (in terms of bonds) atoms of the same molecule. In the event of a heavily bent molecule, these atoms can approach each other and contribute to the energy being calculated. However, in our case it is irrelevant.)

The dimer formation can also been established by the sum of solvent-accessible surface areas (SASA) [27] for both molecules. Clearly that for stuck molecules it should be less than for two isolated ones. This characteristic appeared to be able to determine the time of association of the molecules to the same extent as the E_{LJ} value (Fig. 2). Hereafter, we will use only E_{LJ}.

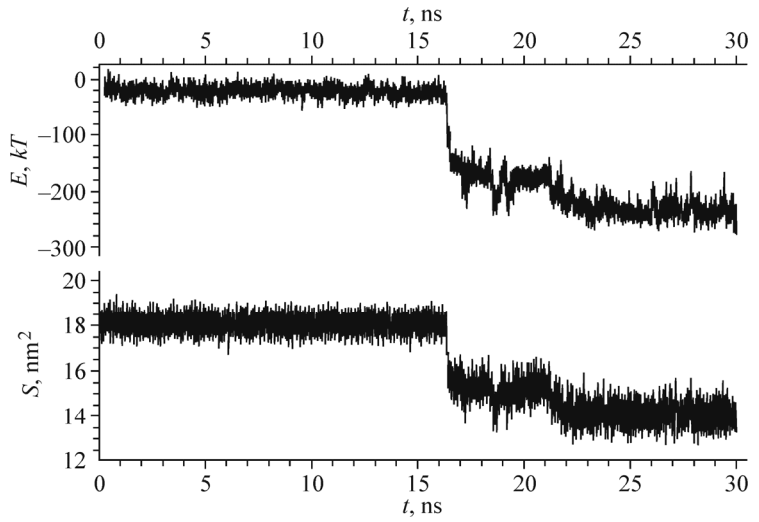

Fig. 2. Determination of the time of appearance of GA dimer in one of the runs of the model with two GA molecules. Top: the energy of Lennard–Jones interaction E_{LJ}, see the text. Bottom, for that same model: the total solvent-accessible surface area (for both GA molecules). The curves experience a jump at approximately 16 ns, which indicates that the molecules have met. The additional jump at 21 ns means the establishment of more optimal molecular contact.

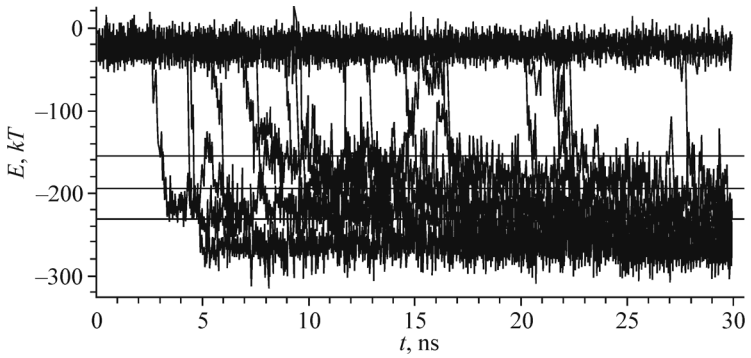

Fig. 3. Time changes in the energy E_{LJ} for all 30 runs of the model with two GA molecules. The horizontal lines mark the 170 *kT*, 210 *kT*, and 250 *kT* energy levels.

Fig. 3 shows the time dependence of E_{LJ} for all 30 runs of the model with two GA molecules. In 20 cases, we observed a sharp decrease in the energy, at different times and by different values. In the other runs, the molecules had never met during the simulation.

By the end of the simulation, the E_{LJ} value for most dimers falls in a range from –200 *kT* to –280 *kT*. In some cases, they formed with this energy almost immediately, while in other runs, the energy decreased in several stages. This points to a complex dynamics of molecular sticking.

Relatively large E_{LJ} values are due to the fact that when GA molecules meet they get a large number of van der Waals contacts. On the other hand, as our additional calculations have shown, this value does not exceed the scale of fluctuations of the total energy of the whole model.

MUTUAL ORIENTATION OF MOLECULES IN THE DIMER

For analyzing the mutual arrangement of GA molecules, we propose to use the vectors associated with a molecule (Fig. 4) and calculate the angles (angle cosines) between these vectors. Therefore, a dimer can be characterized by the following angles:

- The (A1A2) angle between the ***A*** vectors of two GA molecules, which determines the mutual orientation of the terpene skeletons;
- The (B1B2) angle between the ***B*** vectors of sugar ends of the molecules;

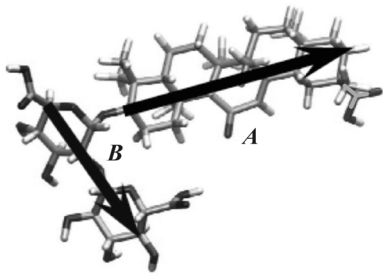

Fig. 4. Molecule of glycyrrhizic acid and the vectors associated with it: the ***A*** vector characterizes the orientation of the terpene skeleton (connects the remote carbon atoms in the terminal rings of the skeleton); the ***B*** vector characterizes the orientation of sugar part (connects the remote atoms in the sugar rings).

- The (A1B1) and (A2B2) angles characterizing the mutual orientation of the skeleton and sugar end within each molecule;
- The (A1B2) and (A2B1) angles, which are the cross angles providing the additional information on the mutual arrangement of molecules.

Figs. 5*a* and 5*b* shows the behavior of these angles on the example of two different runs. In the first case (run 1), GA molecules met and began to stick together in 5 ns after the beginning of the simulation. This can be seen from a jump in the energy E_{LJ}, which is also given in the figures. Then, during the subsequent 5 ns, the molecules adapted to each other. Eventually, a configuration formed, which did not change any more till the end of the simulation.

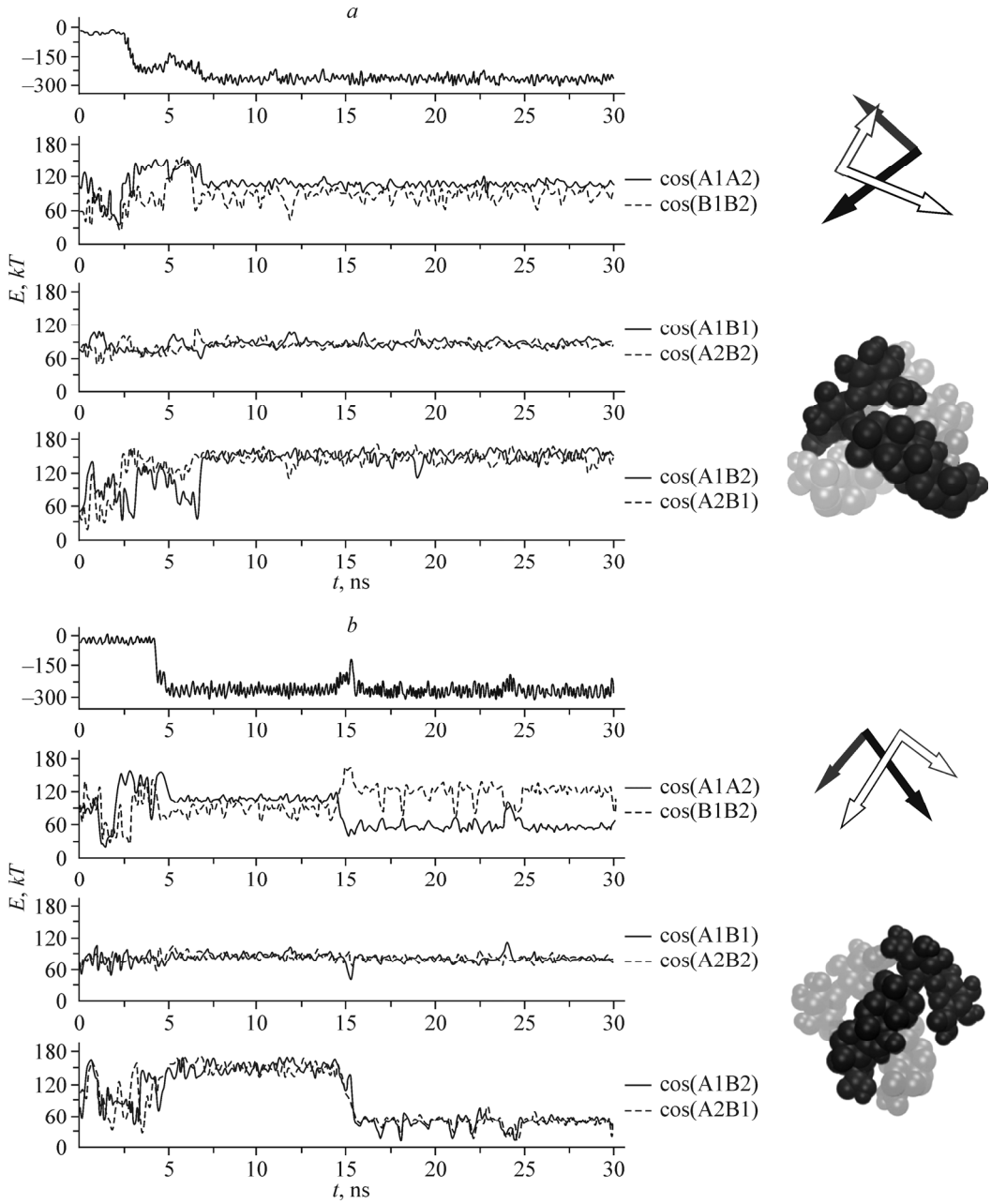

Fig. 5. Energy E_{LJ} and the angles between the vectors of the molecule for run 1 and the scheme of stable dimer and its configuration, extracted from molecular dynamics model (*a*); energy E_{LJ} and the angles between the vectors for run 2 and the structure of dimer formed after 15 ns of the simulation (*b*).

The energy and all angles in it remain almost constant; only small temperature fluctuations are observed. The resulting configuration has the energy $E_{LJ} \approx -265\ kT$. The (A1A2) angle varies within a narrow range (100-110°) being, in average, approximately 105°. Intramolecular (A1B1) and (A2B2) angles are approximately 90° for both models. The (A1B2) and (A2B2) cross angles are also much the same and are about 160°. This means that both molecules in this dimer have the same shape and symmetrically arranged. Fig. 5*a* also shows the scheme of this dimer using the vectors and the configuration extracted from the model.

In run 2, in 5 ns a dimer with the same structure as in run 1 immediately formed. However, here, it existed for only 10 ns, and then a restructuring occurred, which lasted a couple of nanoseconds. This, in particular, is suggested by a small peak on the E_{LJ} curve, which implies a weakening of the Lennard–Jones interaction between the molecules at that point of time. The detailed analysis showed that in this time interval the molecules turned (in the plane of the molecules) approximately by 150°. As a result, the (A1A2) angle became about 50°, and the (B1B2) angle, 120°. The inside angles for both molecules remained the same, 90°. The cross angles are also the same, but now, after the turn, they are approximately 40°. The resulting structure is also symmetrical (Fig. 5*b*). It is noteworthy the outliers on the curve for the (B1B2) angle. They can be explained by the fact that, in this structure, there are no obstacles to the rotational motions of the molecule around an axis coinciding with the terpene skeleton. The surrounding water effects on the sugar ends and thus can initiate these random motions.

Hence, using the vectors associated with GA molecule, we manage to characterize the structure of the dimers. It changes, but there are characteristic types of dimers existing for a long time.

ENSEMBLE OF DIMERS

A detailed analysis of dimers and structural transitions between them requires a special study. Here, we restricted ourselves to the identification of characteristic types in the ensemble of dimers obtained in our simulation.

To exclude those model configurations where the dimer has not yet formed, we discriminate the molecular dynamics path based on the energy E_{LJ} taking into account only those configurations, for which $E_{LJ} < -170\ kT$ (Fig. 3). The condition $E_{LJ} < -210\ kT$ cuts off doubtful configurations identifying the bulk of the resulting dimers, and more stringent condition $E_{LJ} < -250\ kT$ leaves the most "favorable" structures. This task required a special effort, because instantaneous values E_{LJ} strongly fluctuate. We evaluated the instantaneous values E_{LJ} every 0.05 ps. Based on these data, we calculated the moving averages over 100 neighboring values. The obtained smoothed time dependences of E_{LJ} were used to discriminate the molecular dynamics configurations. If, for a given time, the E_{LJ} value satisfied a selected condition, then this configuration was taken to consideration. We used the instantaneous values of the angles. They fluctuation is insignificant, because they reflect the molecular motion as a whole.

Fig. 6*a*, for each selected group of GA dimers, shows the distribution of the (A1A2) angle cosine. The curve includes all 20 runs of this model where the dimers formed. The most favorable dimers ($E_{LJ} < -250\ kT$) are described by only three characteristic values of the angle cosines: –0.9, –0.3, and 0.6, which are close to 150°, 105°, and 55° respectively. Note that the latter two angles were obtained in runs 1 and 2 discussed in Figs. 5*a* and 5*b*. The main set ($E_{LJ} < -210\ kT$) consists of a large number of configurations. The intensity of the mentioned peaks increased, but at the same time, new peaks also appeared in the acute angle area: with the cosine of approximately 0.8 (40°) and near unity (zero angle).

The extension of the set of configurations ($E_{LJ} < -170\ kT$) does not give us new peaks. However, an additional background appears. Put it differently, the GA molecules in ″unstable″ dimers have no well-defined structure. Though, it can be noted that the skeletons of the molecules in these dimers are located rather collinear or anti-collinear than orthogonally.

For a more detailed presentation of the preferred dimer structures, we constructed two-dimensional diagrams where on one axis the (A1A2) angle cosine is plotted, and on the other, the (B1B2) angle cosine. Fig. 7*a* depicts such a diagram showing the occupancy map for the dimers from the main set; i.e., that corresponding to the middle curve in Fig. 6.

The spots marked with the numbers 1, 2, 3 correspond to the main distribution peaks in Fig. 6. Spot 4 corresponds to the peak at cos(A1A2) = 0.8, and spot 5 in the very corner of the diagram corresponds to the peak at cos(A1A2) = 1. Note that the dimer from run 1 discussed above (Fig. 5*a*) refer to the first spot, and dimer from run 2, to the second one.

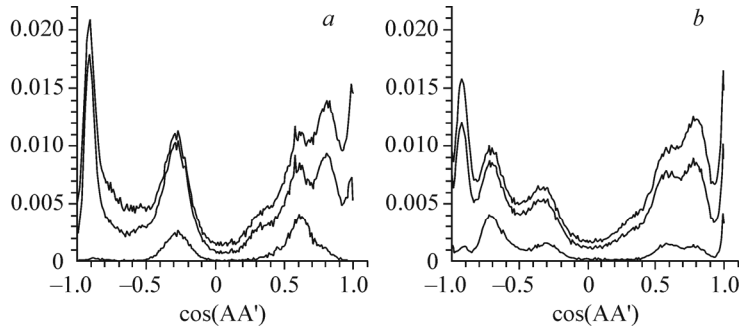

Fig. 6. Distribution of the (A1A2) angle cosine in GA dimers for the model with two GA molecules. Different curves correspond to different boundary values of E_{LJ} used to identify the dimers, top down: $E_{LJ} < -170\ kT$, $E_{LJ} < -210\ kT$, $E_{LJ} < -250\ kT$ (*a*); the same for the model with the inserted cholesterol molecule. In order to select the associates, the Lennard–Jones interaction energy between all three molecules was used. Different curves correspond to the following conditions: $E_{LJ} < -330\ kT$, $E_{LJ} < -390\ kT$, and $E_{LJ} < -430\ kT$ (*b*).

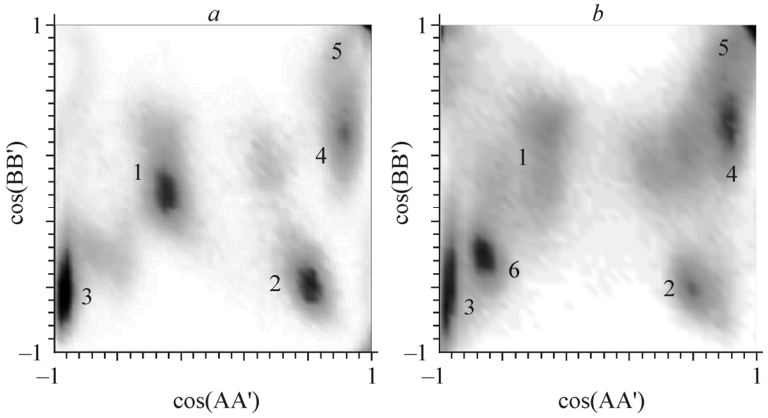

Fig. 7. Distribution of GA dimers (*a*) and 2:1 associates (*b*) in the cos(A1A1)–cos(B1B2) coordinates.

Fig. 8*a* shows the dimers (taken from the molecular dynamics model) corresponding to spots 1-4. It can be seen that each of them represents a closely stuck pair of molecules. There are no voids between them where any other molecule could fit.

ASSOCIATES WITH CHOLESTEROL

Dealing with the second model (two GA molecules and one cholesterol molecule) we identified the associates using the total Lennard–Jones interaction energy E_{LJ} for all three molecules (Fig. 9). The condition $E_{LJ} < -330\ kT$ identifies all 2:1 associates, including those, which have not yet come to equilibrium; the condition $E_{LJ} < -390\ kT$, determines the main set; and the condition $E_{LJ} < -430\ kT$ corresponds to the most low-energy associates.

Again, we characterize the structure of associates using the vectors associated with GA molecules. Fig. 6*b* shows the distribution of the (A1A2) angle cosine between GA molecules in the 2:1 associate. The obtained curves are similar to those for dimers without cholesterol (left). There is only one substantial difference: an additional peak at cos(A1A2) = –0.73. The positions of other peaks match with each other; i.e., the mutual orientation of GA molecules in the associates is about the same as in dimers. As is also obvious from the diagrams in Fig. 7, the main spots are at the same places, but one new spot marked with the number 6 appeared.

This means that the 2:1 associates are generally the dimers of GA, and a cholesterol molecule arranges alongside. A visual confirmation of this is shown in Fig. 8*b*, which depicts the associates extracted from the molecular dynamics paths.

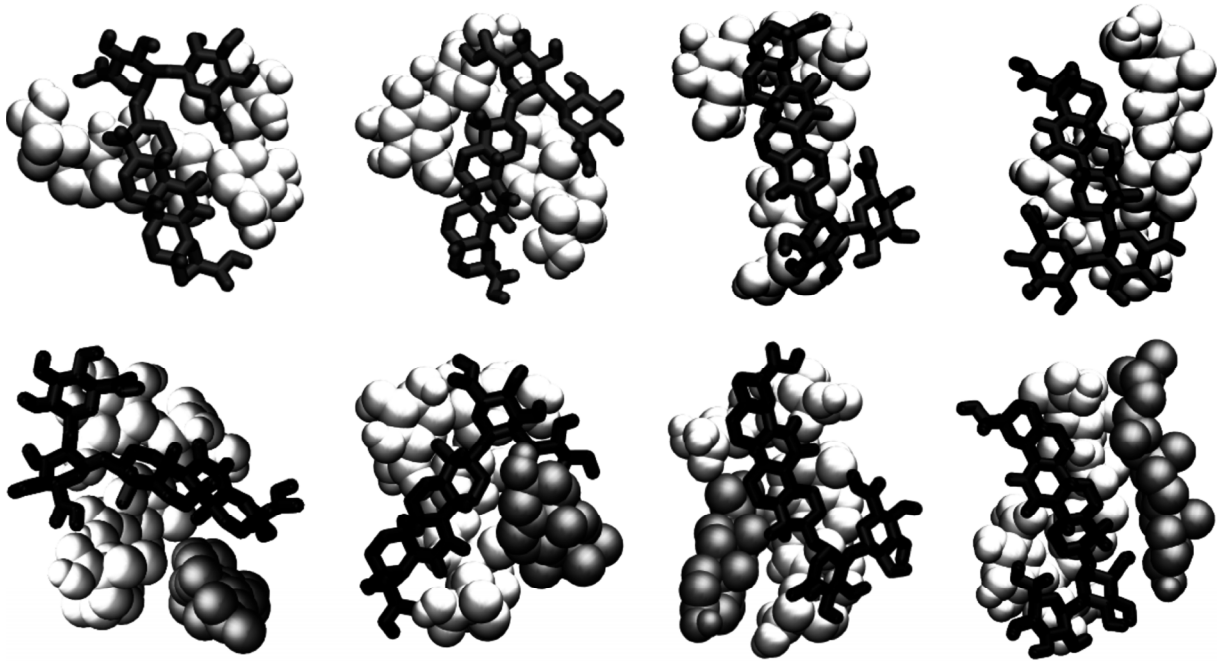

Fig. 8. GA dimers corresponding to spots 1-4 in Fig. 7, *a*. For clarity sake, one of the GA molecules is shown by van der Waals atoms (light grey), and the other, by the skeleton (*a*). Clusters 2:1 are from the respective spots in Fig. 7, *b*. The molecule of cholesterol is shown by dark grey.

The configurations corresponding to spot 6 have a similar structure. Fig. 10 shows such an associate extracted from molecular dynamics model. It also represents a close pair of GA molecules with stuck cholesterol molecule.

This configuration of GA molecules is not a characteristic dimer in our simulation. Nevertheless, in Fig. 8 (left), a nonzero occupation in the area corresponding to spot 6 is seen. It can be thought that the appearance of clear spot 6 in Fig. 8 (right) results from stabilization of the respective configurations by cholesterol. Apparently, the cholesterol molecule somehow influences the mutual arrangement of the neighboring GA molecules. However, there could be another possible reason for appearance of spot 6. We admit that our simulation is not sufficiently representative, i.e., 30 independent runs are not enough to identify all characteristic dimers and accurately estimate their occupancy. In the subsequent runs, yet another types of GA dimers can appear. In this regard, it should be noted that the configurations of GA molecules in the spots marked with the number 1 are somewhat different by the value of the angle between the sugar ends (B1B2). This can be due both to

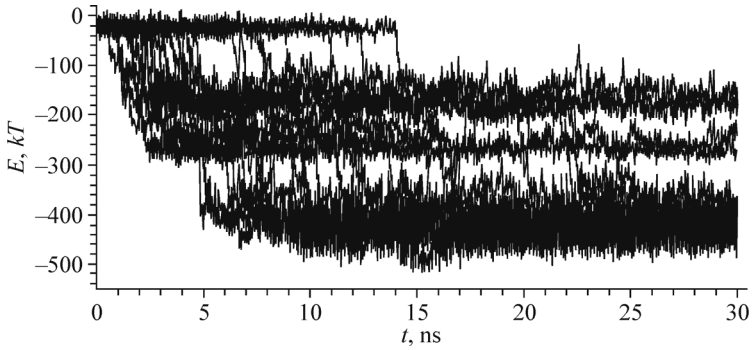

Fig. 9. Behavior of the total energy E_{LJ} for all 30 runs of the model with two GA molecules and one cholesterol molecule. The level of $E_{LJ} \approx -170\ kT$ corresponds to the formation of an associate from one GA molecule and cholesterol; the level of $E_{LJ} \approx -270\ kT$ corresponds to the GA dimer without cholesterol. In the other runs, an aggregate 2:1 formed (the curves below –330 *kT*).

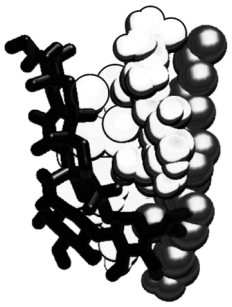

Fig. 10. Structure of the 2:1 associate from spot 6 in Fig. 8 (right). The molecule of cholesterol is located to the right.

the effect of cholesterol on the structure of a known dimer and the appearance of dimers with somewhat different structure. Elucidation of these issues requires additional calculations and is not the purpose of this paper.

In this work, we point out that a 2:1 associate can be considered as a close pair of GA molecules (as a rule, corresponding to one of characteristic dimers) with the attached cholesterol molecule. Therewith, it should be emphasized that the pair of GA molecules in water solution does not form a ″ring″ able to encompass the cholesterol molecule.

CONCLUSIONS

We performed the molecular dynamics simulation of aqueous solutions of GA containing two GA molecules in the model box and the solutions, in which a cholesterol molecule was inserted. We examined the GA dimers and the 2:1 associates consisting of two GA molecules and one cholesterol molecule. The dimers and associates formed are sufficiently stable: during the simulation we have never seen the aggregated molecules to decouple. At the same time, the molecules in the cluster remain mobile and can change their mutual orientation.

We identified relatively stable types of dimers differing in the mutual arrangement of terpene skeletons and sugar ends. These structures are advantageous due to more favorable hydrophobic contacts between GA molecules. The GA molecules in the dimer are always located compactly; i.e., there is no place between them where another molecule, including water molecule, could fit. The 2:1 associates are a close pair of GA molecules, which, as a rule, corresponds to one of characteristic dimers, and the cholesterol molecule attaches to this pair arranging alongside.

It should be emphasized that the system (two GA molecules in the box) calculated here models the situation of low GA concentrations. As it was shown in many physicochemical studies [3-12] and tests on laboratory animals [2], it is precisely these premicellar GA aggregates that form the most stable complexes with slightly soluble medicinal compounds and provide the greatest therapeutic effect. Based on the results obtained in this paper, it can be suggested that the observed effects are associated with an increase in the solubility of medicinal compounds in a complex with GA.

The work was supported by the RFBR grants No. 12-03-31183-mol and No. 12-03-00654a and by the grant RUC-7067-NO-12 from the U.S. Civilian Research & Development Foundation (CRDF Global).

REFERENCES

1. G. A. Tolstikov, L. A. Boltina, R. M. Kondratenko, et al., *Glycyrrhiza: Biodiversity, Chemistry, and Application in Medicine* [in Russian], NP “Geo”, Academic Publishing House, Novosibirsk (2007).
2. T. G. Tolstikova, M. V. Khvostov, and A. O. Bryzgalov, *Mini-Rev. Med. Chem.*, **9,** 1317-1328 (2009).
3. N. E. Polyakov and T. V. Leshina, *Open Conf. Proc. J.*, **2,** 64-72 (2011).
4. V. A. Vavilin, N. F. Salakhutdinov, Yu. I. Ragino, N. E. Polyakov, M. B. Taraban, T. V. Leshina, E. M. Stakhneev, V. V. Lyakhovich, Yu. P. Nikitin, and G. A. Tolstikov, *Biomed. Chem*., **54,** 301-313 (2008).
5. Yu. I. Ragin, V. A. Vavilin, N. F. Salakhutdinov, S. I. Makarov, E. M. Stakhneva, O. G. Safronova, Yu. P. Nikitin, and G. A. Tolstikov, *Bull. Exp. Biol. Med*., **145,** 285-287 (2008).
6. N. E. Polyakov, V. K. Khan, and M. B. Taraban, *J. Phys. Chem. B*, **109,** 24526-24530 (2005).
7. N. E. Polyakov, T. V. Leshina, N. F. Salakhutdinov, et al., *J. Phys. Chem. B,* **110,** 6991-6998 (2006).
8. N. E. Polyakov, T. V. Leshina, N. F. Salakhutdinov, et al., *Free Rad. Biol. Med*., **40,** 1804-1809 (2006).
9. N. E. Polyakov, V. K. Khan, M. B. Taraban, et al., *J. Phys. Chem. B*, **112,** 4435-4440 (2008).
10. N. E. Polyakov, A. Magyar, and L. D. Kispert, *J. Phys. Chem. B*, **117**, No. 35, 10173-10182 (2013).
11. V. S. Kornievskaya, A. I. Kruppa, N. E. Polyakov, and T. V. Leshina, *J. Incl. Phenom. Macrocycl. Chem*., **60,** 123-130 (2007).
12. K. C. James and J. B. Stanford, *J. Pharm. Pharmacol*., **5,** 445-450 (1962).
13. R. J. Gilbert and K. C. James, *J. Pharm. Pharmacol*., **16,** 394-399 (1964).

14. E. Azaz and R. Segal, *Pharm. Acta Helv*., **55,** 183-186 (1980).
15. M. Kondo, H. Minamino, and G. Okiyama, *J. Soc. Cosmet. Chem*., **37,** 177-189 (1986).
16. M. Maskan, *J. Food Process Eng*., **39,** 389-393 (1999).
17. T. V. Romanenko and Yu. I. Murinov, *J. Phys. Chem*., **75,** 1601-1604 (2001).
18. O. Yu. Gluschenko, N. E. Polyakov, and T. V. Leshina, *Appl. Magn. Res*., **41,** 283-294 (2011).
19. T.-T. Chang, M.-F. Sun, K.-C. Chen, et.al., *Molec. Simulat*., **37**, No. 9, 804-811 (2011).
20. A. V. Lekar, A. A. Milov, S. N. Borisenko, et al., *Vestn. Yuzhn. Nauch. Tsentra RAN*, **8**, No. 2, 18-26 (2012).
21. D. Van der Spoel, E. Lindahl, B. Hess, G. Groenhof, A. E. Mark, and H. J. C. Berendsen, *J. Comput. Chem*., **26**, No. 16, 1701-1718 (2005).
22. W. G. Hoover, *Phys. Rev. A*, **31,** 1695-1697 (1985).
23. M. Parrinello and A. Rahman, *J. Appl. Phys*., **52,** 7182 (1981).
24. U. Essmann, L. M. Perera, L. Berkowitz, T. A. Darden, H. Lee, and L. G. Pedersen, *J. Chem. Phys*., **103,** 8577-8593 (1995).
25. A. K. Malde, L. Zuo, M. Breeze, M. Stroet, D. Poger, P. C. Nair, C. Oostenbrink, and A. E. Mark, *J. Chem. Theory Comput*., **7**, No. 12, 4026-4037 (2011).
26. http: // www.compbio.biosci.uq.edu.au/atb/.
27. F. M. Richards, *Methods Enzymol*., **115,** 440-646 (1985).